Increased outburst flood hazard from Lake Palcacocha due to human-induced glacier retreat

R. F. Stuart-Smith [1,2 ✉], G. H. Roe[2], S. Li[1,3] and M. R. Allen [1,4]

A potential glacial lake outburst flood from Lake Palcacocha (Cordillera Blanca, Peru) threatens Huaraz, a city of 120,000 people. In 1941, an outburst flood destroyed one-third of the city and caused at least 1,800 fatalities. Since pre-industrial times, Lake Palcacocha has expanded due to the retreat of Palcaraju glacier. Here we used observations and numerical models to evaluate the anthropogenic contribution to the glacier's retreat and glacial lake outburst flood hazard. We found that the magnitude of human-induced warming equals between 85 and 105% (5–95% confidence interval) of the observed 1 °C warming since 1880 in this region. We conclude that it is virtually certain (>99% probability) that the retreat of Palcaraju glacier to the present day cannot be explained by natural variability alone, and that the retreat by 1941 represented an early impact of anthropogenic greenhouse gas emissions. Our central estimate is that the overall retreat is entirely attributable to the observed temperature trend, and that the resulting change in the geometry of the lake and valley has substantially increased the outburst flood hazard.

The worldwide retreat of mountain glaciers is one of the most prominent impacts of climate change in public discourse and an established consequence of anthropogenic climate change[1-3], with Andean glaciers among the fastest retreating[3,4]. Mountain glacier lengths have decadal-to-multidecadal response times[5,6] and act as lowpass filters of climate[6,7]. They therefore represent a purer signal of anthropogenic climate change than most other metrics. However, any individual glacier's response to climate change depends on its geographical and climatic setting[1,2,8]. An assessment of the human contribution to an individual glacier's retreat and hence changing glacial lake outburst flood (GLOF) hazard must quantify these factors and place the observed change in the context of the natural variability expected in the absence of anthropogenic climate change.

GLOFs are a dangerous hazard in deglaciating alpine environments, and downstream inundation from large outburst floods have caused serious damage to human settlements[9] and infrastructure[10]. GLOFs can occur from englacial, subglacial, supraglacial and proglacial lakes. GLOFs from proglacial lakes that form in the wake of a retreating glacier, such as Lake Palcacocha, are a response to the disequilibrium imposed on glacial landscapes by climate change[11,12]. They occur when an unstable moraine dam is breached or a moraine-overtopping wave is induced by a triggering event, such as a landslide or an avalanche[13]. However, the anthropogenic influence on a specific GLOF has hitherto not been evaluated[9]. In the mid twentieth century, new proglacial lakes formed throughout the Cordillera Blanca as glacier termini receded[14] and multiple fatal GLOFs were recorded, including those from Lakes Ayhuinyaraju, Jancururish, Tumarina and Palcacocha[15]. The ongoing GLOF hazard continues to require extensive mitigation and engineering efforts[16,17]. We focus here on Lake Palcacocha, which currently threatens the city of Huaraz with a GLOF[3,11-13,16,18,19].

Lake Palcacocha (9° 23′ 49″ S 77° 22′ 47″ W) sits at the foot of Palcaraju glacier. Lichenometric dating of Palcaraju glacier's terminal moraine indicates a seventeenth century formation, which sets the maximum extent of the glacier in the past few centuries[15,20].

Photographic records of Palcaraju glacier (Fig. 1) show the 1939 terminus set well back from the terminal moraine, with an overspilling Lake Palcacocha between the glacier's terminus and terminal moraine. In 1941, the breaching of Lake Palcacocha's moraine dam resulted in the Cordillera Blanca's deadliest GLOF of the twentieth century[15]. The resulting debris flow destroyed one-third of Huaraz and killed at least 1,800 people[12,14,21]. A limited expansion of Lake Palcacocha was observed between 1948 and 1995, and the lake area increased from 0.06 to 0.08 km². The rapid retreat of Palcaraju glacier since 1995 expanded the lake to an area of 0.49 km² in 2018[22]. Two concrete overflow spillways were installed in the terminal moraine between 1972 and 1974. Up to 2011, the lake surface elevation remained constant and the lake volume grew as Palcacocha expanded into the space previously occupied by the retreating glacier. In 2011, siphons were installed to lower the water surface by 3–5 m, although the GLOF hazard remains high[12]. The most recent bathymetric survey found that the volume of Lake Palcacocha was 17,403,353 m³ in 2016[23], a 34-fold increase from the volume of the post-GLOF lake in 1941, which makes it the fourth largest of the 35 glacial lakes with installed safety features in the Cordillera Blanca[16].

Any evaluation of the contribution of anthropogenic greenhouse gas and aerosol emissions to a changing GLOF hazard must consider the whole causal chain. Our study has three parts. We evaluated: (1) the anthropogenic contribution to the observed temperature trend, (2) the role of this trend in the observed retreat of Palcaraju glacier (which comprises numerical modelling of the glacier and a statistical comparison of the observed retreat with the natural length variability) and (3) the role of the glacier's retreat in reshaping the valley and the resultant change in the GLOF hazard.

Attribution of Peru's temperature trend to human activity

Globally, virtually all long-term temperature variations since the mid-nineteenth century have been attributed to external forcing[24]. Following the approach taken by Haustein et al.[25] and for Fig. 1.3 in Allen et al.[26], we obtained the local annual mean temperature (Methods) from the relevant grid cell in the HadCRUT4-Cowtan/

[1]Environmental Change Institute, University of Oxford, Oxford, UK. [2]Department of Earth and Space Sciences, University of Washington, Seattle, WA, USA. [3]Oxford e-Research Centre, Department of Engineering Science, University of Oxford, Oxford, UK. [4]Department of Physics, University of Oxford, Oxford, UK. ✉e-mail: rupert.stuart-smith@ouce.ox.ac.uk
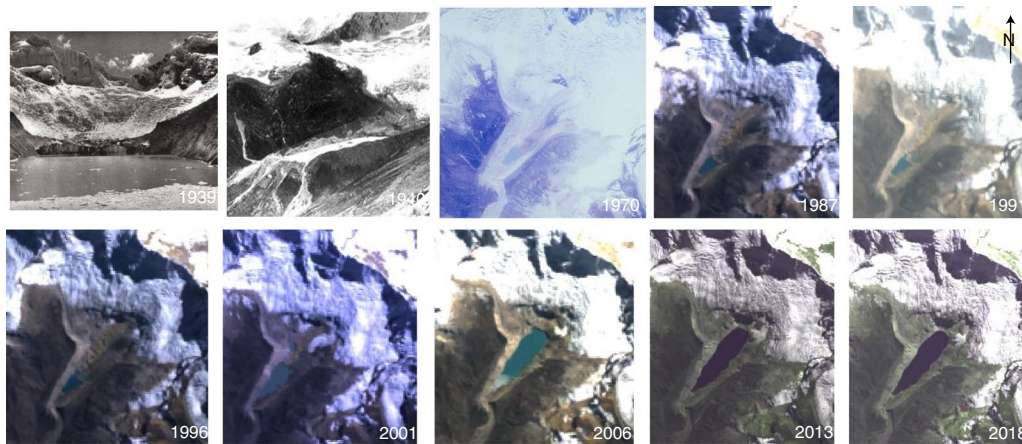
Fig. 1 | In situ (1939, 1940 and 1970) and satellite (1987 onwards) images showing the evolution of Lake Palcacocha. a–j, In situ (**a–c**) and satellite (**d–j**) images of Lake Palcacocha. This shows an overspilling lake prior to the 1941 GLOF and then an initially minimal expansion followed by rapid lake growth due to the retreat of the glacier. Images in **c–j** were taken in July/August. Images reproduced with permission from ref. [49], Hans Kinzl (**a,b**); USGS (EROS Archive) (**c**); USGS Earth Explorer Landsat 5 (**d–h**) and Landsat 8 (**i, j**).
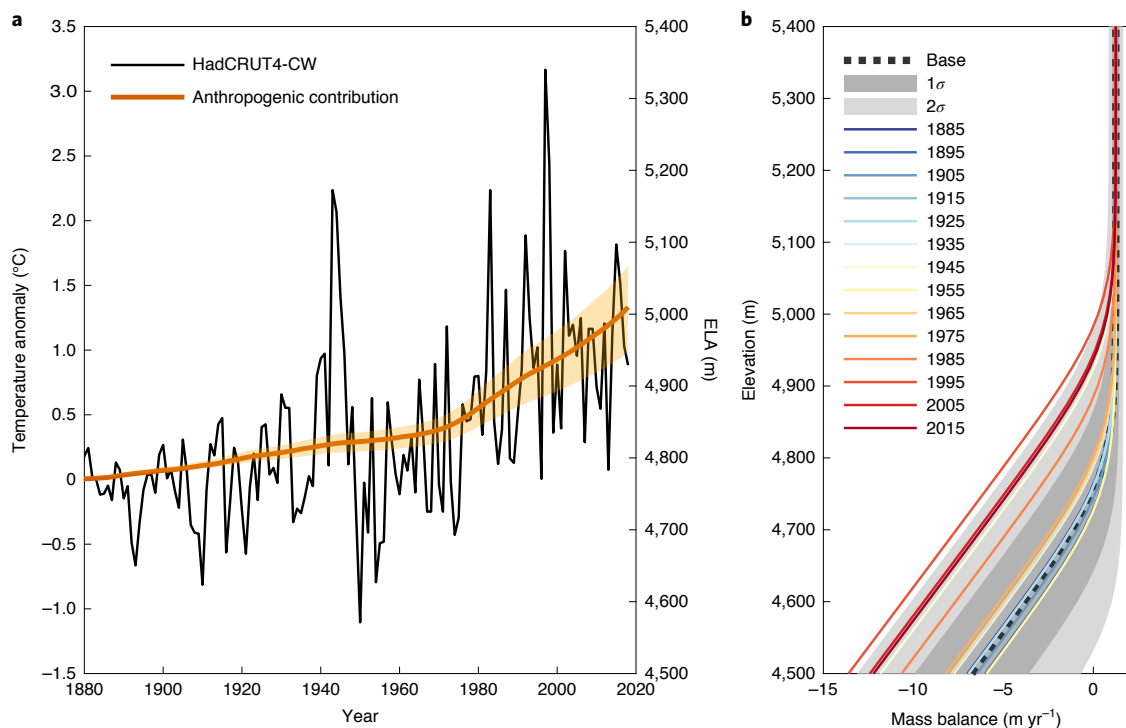

Fig. 2 | Regional observed and attributable temperature anomalies, and impacts on decadal mean mass-balance profile. a, Annual mean temperature (HadCRUT4-CW) expressed as anomalies from 1850 to 1880 and the resulting ELA, and the contribution of anthropogenic forcing to the observed temperature change, with its 5–95% uncertainty ranges (shaded orange). **b,** The resulting mass-balance profiles, plotted as decadal means, with the 1σ and 2σ mass-balance range around the base profile shown in grey. The glacier's 1880 profile (Fig. 3) is in mass balance for the base profile.

Way (HadCRUT4-CW) dataset[27,28] (Fig. 2a). The HadCRUT4-CW trend is well supported by regional observations (Methods). To quantify the anthropogenic contribution to regional temperature change, we regressed the observed temperatures in HadCRUT4-CW onto the Global Warming Index (GWI)[25], an estimate of the anthropogenic contribution to global externally forced temperature change, over the period 1940–2018 (Methods). This yielded region-specific scaling factors for the GWI. Regional anthropogenically forced warming is the product of this scaling factor and the GWI anomaly relative to 1880. For 1989–2018, it was found to

be equal to 95% (85–105%, 5–95% range, all percentages rounded to the nearest 5%) of the observed temperature change over the same period. Uncertainty bounds are given by the intermodel range of regressions of the relevant grid cell in the control runs (with non-evolving pre-industrial conditions) of the Coupled Model Intercomparison Project Phase 5 (CMIP5) against the GWI. Figure 2a shows the observed temperature change for the HadCRUT4-CW grid cell that contains Palcaraju glacier (black) and the temperature change in the same grid cell attributed to human greenhouse gas and aerosol emissions (orange). The correlation
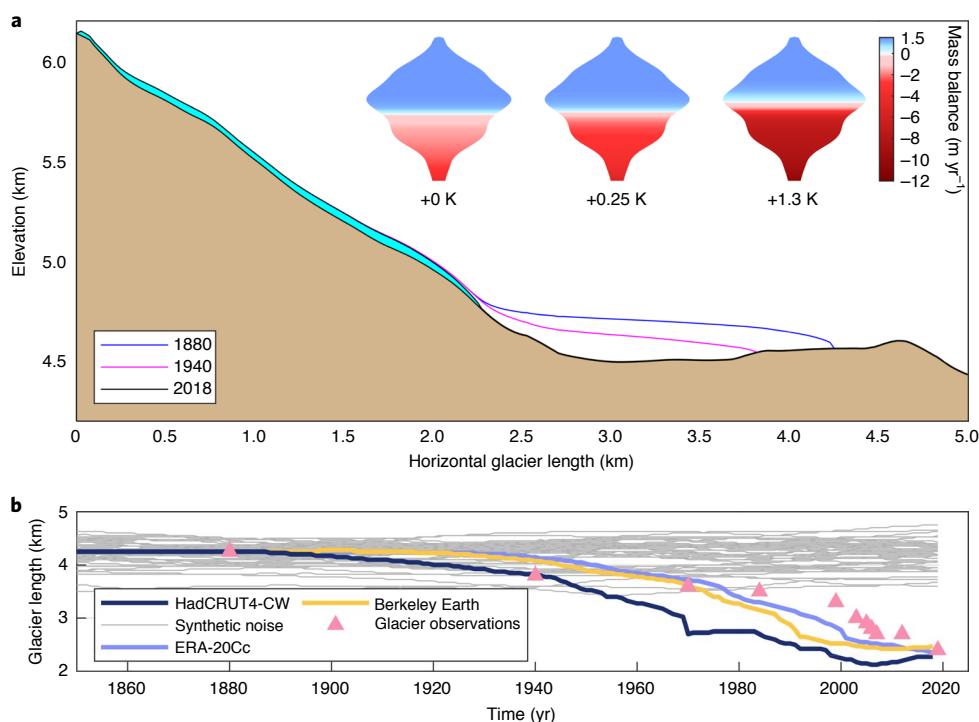
Fig. 3 | Mass-balance response to temperature change and modelled and observed retreat of Palcaraju glacier. a, Longitudinal profile of Palcaraju glacier in 1880 (blue), 1940 (magenta) and 2018 (cyan) in the HadCRUT4-CW flowline model simulation. Inset: idealized plan view of the glacier catchment with the glacier width symmetrized about the flowline (approximately 5 km across at its widest point) and the mass-balance profile for the baseline, +0.25 K and +1.3 K climates, which correspond to the anthropogenic warming in 1880, 1940 and 2019, respectively. **b**, The modelled glacier length for three temperature time series (for which the temperature changes begin in 1880, 1890 and 1900 for HadCRUT4-CW, Berkeley Earth and ERA-20C, respectively; Methods), compared with the estimated 1880 glacier terminus position and observed 1940–2019 positions (interpreted from aerial imagery, shown as magenta triangles) and synthetic natural glacier length variability (grey lines). Retreat since 1850 is estimated to be 1825 m in the observations, compared with the modelled values of 1950 m (HadCRUT4-CW), 1750 m (Berkeley Earth) and 1875 m (ERA-20C).

between regional temperatures and global anthropogenic warming with the estimated response to the natural external climate drivers (solar variability and volcanic activity) is negligible.

Attribution of the Palcaraju glacier retreat to climate change

The climate that a glacier experiences can be characterized by the vertical profile of its mass balance (that is, accumulation minus ablation)[29]. We used a mass-balance profile (Fig. 2b) for Palcaraju glacier, which, for the current climate, matches that observed on Shallap glacier (9° 29′ 24″ S, 77° 20′ 24″ W, a well-observed glacier approximately 10 km away, with similar aspect to that of Palcaraju)[29]. The equilibrium line altitude (ELA, ~4,950 m in the current climate) denotes the altitude above which there is net accumulation and below which there is net ablation. A simple and robust method to quantify the impact of climate change on glacier mass balance is via geometrical shifts of the mass-balance profile in response to temperature and precipitation changes[30–33]. The climatological precipitation is important for the shape of the mass-balance profile but, on century timescales, precipitation trends are small and temperature changes dominate the mass-balance changes[32,34] (see also Methods and Supplementary Information). Temperature changes are implemented through a vertical shift of the ELA based on the temperature lapse rate (here, approximately 5.5 K km⁻¹, which gives an ELA sensitivity of approximately 180 m K⁻¹) (refs. [32,35]). Detailed surface-energy-balance models show a close agreement with this value for glaciers in the Cordillera Blanca[32,36].

Figure 2b shows the decadal mean mass-balance profiles produced in response to the HadCRUT4-CW observations since 1880.

Tropical glaciers are characterized by steep vertical gradients in ablation, which renders them particularly sensitive to climatic perturbation[35]. Starting from an 1880 baseline, the point at which anthropogenic warming begins to emerge (Fig. 2a), warmings of 0.25 and 1.3 K (the respective anthropogenic contributions in 1941 and 2019) raise the ELA by 45 and 235 m, respectively. At an elevation of 4,600 m, characteristic of the early twentieth century ablation zone, these temperature changes increase the net ablation rate by 30 and 150%, respectively. Given the linear relationship between temperature and ELA, human-induced warming (as previously stated) and the change in ELA are equal to 95% of the observed temperature and modelled ELA changes, respectively.

Next, we used a numerical flowline model of ice dynamics (Methods) to evaluate the thickness profiles of the glacier during its retreat, the interaction of a rising ELA with the valley geometry and the natural glacier fluctuations in the absence of climate change. In the absence of direct observations, we estimated that the nineteenth century glacier terminus was situated 4.25 km along the flowline (Methods). Uncertainty in the 1880 terminus position has no effect on the present-day terminus position due to the geometry of the valley and the short response time of the modern glacier (Supplementary Information and Supplementary Fig. 1).

We modelled the response of Palcaraju glacier to regional annual temperature anomalies from three sources: HadCRUT4-CW (Fig. 2a), Berkeley Earth Land/Ocean observations[37] and the European Centre for Medium-Range Weather Forecasts' twentieth century reanalysis (ERA-20C)[38].

For all three temperature time series, the numerical model gives an overall retreat similar to that observed (Fig. 3a,b), with the

timing of the period of most rapid retreat being less predictable. The planform insets in Fig. 3a show the regions of the glacier with net accumulation in blue and net ablation in red, and highlight that this non-linear retreat is a geometrical consequence of the steep vertical gradient in mass balance and shallow slopes in the lower valley. Applied to the 1880 profile, a warming of 0.25 K causes the net ablation below the ELA to increase by 40%, from 1.8 m yr^{-1} to 2.5 m yr^{-1}, which cannot then be balanced by the 1.1 m yr^{-1} of net accumulation above the ELA. For 1.3 K of warming, the average net ablation rate increases by 230% to 5.9 m yr^{-1}, and there is a 10% decrease in net accumulation above the ELA to 1.0 m yr^{-1}. Rising temperatures have expelled the glacier from the lower valley.

In the observations and our simulations, the glacier retreats rapidly between lengths of approximately 3.0 and 2.7 km, taking four years in observations, and one, six and six years in our modelled response to the HadCRUT4-CW, Berkeley Earth and ERA-20C, respectively, time series. This period of rapid retreat is present in all the simulations, although its timing is sensitive to the warming history. It occurs in our model when thin ice above the slope break completely ablates to isolate a patch of stagnant ice on the lower slope. For the real glacier, the timing and nature of this retreat also depends on the glacier–lake interactions and other processes not represented in our simulations. Our numerical model lacks lake–ice dynamics (which include glacier calving and thermal conduction) and debris cover (Methods), which probably affects the match between the transient evolution of the observed and modelled termini (Fig. 3b).

Could the observed retreat have happened without anthropogenic global climate change? Interannual climate variability will cause glacier fluctuations even in the absence of large-scale climate change[6,39]. The standard deviations (1σ) of regional annual mean temperature and precipitation are approximately 0.5 K and 0.2 m yr^{-1}, respectively, with some interannual persistence, probably due to the influence of El Niño (Methods). Applying this climatic variability to the 1880 glacier profile in the flowline model gives an interannual variability in ELA and mass balance of 100 m and 0.75 m yr^{-1}, respectively (both 1σ), consistent with observations of similar glaciers[40]. We generated 10 kyr of synthetic climate variability and found centennial-scale length fluctuations with a standard deviation (σ_L) of 230 m (Figs. 3b and 4a). Figure 4b,c shows histograms of the trends over 60 and 140 years from the model output, compared with the observed retreat of Palcaraju between 1880 and 1940 or 2018, estimated at 550 and 1,850 m, respectively. In both cases the rates of observed retreat are larger than any of the model output, which indicates that a large-scale climate change is a necessary condition for the glacier's observed length change to occur.

We then quantified the change in glacier length that can occur from natural variability alone ($\Delta L|_{null}$), which includes uncertainty in the glacier response time (τ) and the standard deviation of the glacier length (σ_L). This analysis accounts for glaciers' amplification of the signal-to-noise ratio of climate change[2] (Fig. 4d and equation (4); Methods) and generates probability density functions (PDFs) for trends over 60 and 140 years in the absence of climate change (Fig. 4e,f; Methods). Given our assumptions, we conclude that it is virtually certain (>99% probability) that the observed retreat of Palcaraju glacier could not have occurred due to natural variability alone and therefore that the observed large-scale climate warming that we attribute to human influence is a 'necessary cause'[41] of the observed retreat, both to 1940 and to the present.

The PDF of $\Delta L|_{null}$ is symmetrical and centred over 0 m. Thus, over a 140 year period, the probability that the glacier would have extended is equal to the probability that it would have retreated, so our central (mean and median) estimate for $\Delta L|_{null}$ is 0 m. Consequently, our central estimate for the attributable fraction of the observed retreat to the observed temperature trend is 100%.

Above, we show that anthropogenic warming equals 95% of the observed temperature change in 1989–2018.

Further, for the 1940 retreat not to have been the result of early anthropogenic warming (and be explained only by natural variability) at the 90% confidence level, the pre-anthropogenic equilibrium terminus must have lain within 200 m of the observed 1940 position (Fig. 4e and Supplementary Fig. 2d). This is inconsistent with the early twentieth century retreat observed elsewhere in the Cordillera Blanca and the glacier-length sensitivity to climate change required for the formation of the seventeenth century moraine (Methods, and refs. [14,42–44]). It would also require some unknown factor to counter the impact of the 0.25 K of anthropogenic warming on the mass balance (Fig. 3a inset).

Implications for a GLOF hazard

Our results establish that the present geometries of the glacier and lake are the result of anthropogenic climate change. What are the implications for a GLOF hazard? A GLOF hazard is the product of the probability of a GLOF event occurring and the event magnitude[45]. Previous work has shown that, although a catastrophic breach of the moraine dam is unlikely, the present GLOF hazard from Lake Palcacocha is very high due to the substantial likelihood of an avalanche or landslide inducing a moraine-overtopping wave[12,19]. We used two ranking methodologies to evaluate changes in the GLOF hazard from Lake Palcacocha between the present day and the nineteenth century (Methods and Supplementary Tables 2 and 3). The ranking schemes indicate that the greatest influences on the increasing GLOF hazard are the steepness of the glacier snout, the growing lake area and the glacier's retreat. The geometrical method of Wang et al.[46] was developed for settings in which a moraine-overtopping wave is the likely GLOF mechanism[46]. In line with previous applications of this methodology to Palcacocha[11], we confirmed that the present GLOF hazard is categorized as 'very high' and found that it has increased from 'medium' in the nineteenth century. We compared these results with a geomorphological assessment methodology adapted from Bolch et al.[47]. This also ranks Lake Palcacocha in the highest GLOF hazard category, with the nineteenth century GLOF risk categorized as 'medium'. As a result of this increase in GLOF hazard, Lake Palcacocha is considered a serious threat to Huaraz, which compels the local authorities to implement hazard mitigation measures[19].

The retreat of Palcaraju glacier, and the resultant expansion of Lake Palcacocha, has increased both the probability and potential magnitude of a GLOF. In addition to the criteria assessed by the two hazard assessment methodologies employed here, permafrost degradation in response to rising temperatures can decrease slope stability, which increases the probability of rockfalls and landslides into glacial lakes. Further, the retreat of glaciers, such as Palcaraju, to steep mountain headwalls brings proglacial lakes closer to icy mountain flanks that have decreased stability due to glacier de-buttressing[47,48]. The increase in lake size since the nineteenth century has also increased the likely GLOF volume, although neither methodology accounts for this change (the methodology of Bolch et al.[47] includes area, but the lake is already in the highest area class in the nineteenth century).

The GLOF hazard posed by Lake Palcacocha to Huaraz has increased substantially due to the lake's expansion as Palcaraju glacier retreats and has now become a critical threat to Huaraz, which requires engineered mitigation efforts. Given the assumptions in this three-step attribution, we found: (1) anthropogenic warming equals 95% (85–105%, 5–95% confidence interval) of the observed warming in 1989–2018, (2) our central estimate is that the retreat of Palcaraju glacier is entirely the result of this warming, (3) the retreat cannot be explained by natural climatic variability alone and (4) this retreat has substantially increased the GLOF hazard for Huaraz. Despite some uncertainty about the 1880 position of the glacier
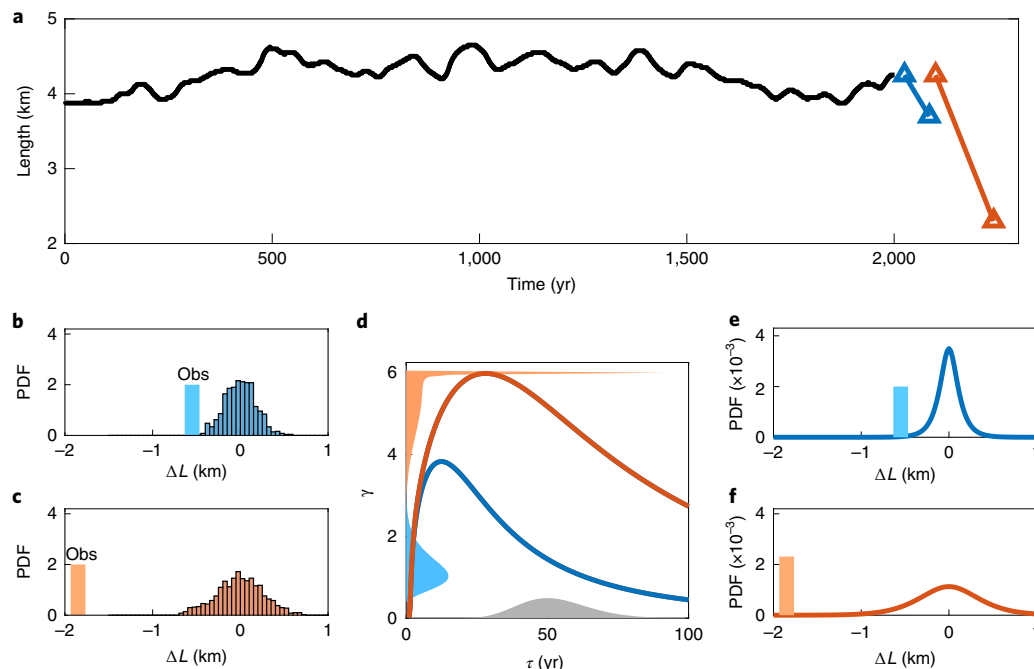
Fig. 4 | Analysis of the signal-to-noise ratio for Palcaraju glacier. a, A 2 kyr sample of glacier-length fluctuations that occurred due to natural mass-balance variability alone (that is, no temperature trend) taken from a 10 kyr simulation (black) and compared with the observed retreat of Palcaraju glacier 1880–1940 (blue) and that of 1880–2019 (orange). **b**, Histogram of the modelled changes over 60 yr in the 10 kyr simulation of natural variability, as compared with the retreat observed (Obs) between 1880 and 1940. **c**, As **b**, but over 140 yr and compared with the observed length change between 1880 and 2019. **d**, Transfer functions (solid lines) used to calculate a glacier's amplification factor (γ) for temperature trends over 60 yr (blue) and 140 yr (orange), based on the glacier's nineteenth century τ (ref. [2]). We accounted for uncertainty in the value of τ in 1880 in the PDF on the horizontal axis (grey shading), which gives rise to a PDF of values for γ for each of the time periods (shaded PDFs on the vertical axis). **e**, The PDF for $\Delta L|_{\text{null}}$ in any 60 yr period in a climate with interannual temperature variability but no climate change trend, compared with the observed retreat between 1880 and 1940 (vertical bar). **f**, As **e**, but for a 140 yr period and as compared with 1880–2019.

terminus, our analysis also provides strong evidence of anthropogenic influence on the 1941 GLOF, a mid-twentieth century humanitarian catastrophe. For the attribution of the overall retreat of Palcaraju glacier, the nineteenth century position of the terminus is of lesser importance, and the present-day threat to Huaraz is a direct consequence of the anthropogenically driven retreat of Palcaraju glacier.

Our analyses demonstrate the utility of risk-based approaches to evaluate the anthropogenic contribution to slow-onset, persistent hazards. The set of analyses presented in this article could be applied to assess anthropogenic influence on the GLOF hazard in any deglaciating alpine environment. Application of these methods in other locations would provide regional and global insight into the human influence on present GLOF hazards and indicate how a GLOF hazard may evolve under future climate change and where adaptation measures may need to be implemented.

Online content

Any methods, additional references, Nature Research reporting summaries, source data, extended data, supplementary information, acknowledgements, peer review information; details of author contributions and competing interests; and statements of data and code availability are available at https://doi.org/10.1038/s41561-021-00686-4.

References

1. Zemp, M. et al. Historically unprecedented global glacier decline in the early 21st century. *J. Glaciol.* **61**, 745–762 (2015).
2. Roe, G. H., Baker, M. B. & Herla, F. Centennial glacier retreat as categorical evidence of regional climate change. *Nat. Geosci.* **10**, 95–99 (2017).
3. Hock, R. et al. in *IPCC Special Report on the Ocean and Cryosphere in a Changing Climate* (eds Pörtner, H.-O. et al.) 131–202 (WMO, 2019).
4. Dussaillant, I. et al. Two decades of glacier mass loss along the Andes. *Nat. Geosci.* **12**, 802–808 (2019).
5. Jóhannesson, T., Raymond, C. & Waddington, E. Time-scale for adjustment of glaciers to changes in mass balance. *J. Glaciol.* **35**, 355–369 (1989).
6. Roe, G. H. & O'Neal, M. A. The response of glaciers to intrinsic climate variability: observations and models of late-Holocene variations in the Pacific Northwest. *J. Glaciol.* **55**, 839–854 (2009).
7. Oerlemans, J. Holocene glacier fluctuations: is the current rate of retreat exceptional? *Ann. Glaciol.* **31**, 39–44 (2000).
8. Sagredo, E. A. & Lowell, T. V. Climatology of Andean glaciers: a framework to understand glacier response to climate change. *Glob. Planet. Change* **86–87**, 101–109 (2012).
9. Harrison, S. et al. Climate change and the global pattern of moraine-dammed glacial lake outburst floods. *Cryosphere* **12**, 1195–1209 (2018).
10. Schwanghart, W., Worni, R., Huggel, C., Stoffel, M. & Korup, O. Uncertainty in the Himalayan energy–water nexus: estimating regional exposure to glacial lake outburst floods. *Environ. Res. Lett.* **11**, 074005 (2016).
11. Emmer, A. & Vilímek, V. Review article: lake and breach hazard assessment for moraine-dammed lakes: an example from the Cordillera Blanca (Peru). *Nat. Hazards Earth Syst. Sci.* **13**, 1551–1565 (2013).
12. Somos-Valenzuela, M. A., Chisolm, R. E., Rivas, D. S., Portocarrero, C. & McKinney, D. C. Modeling a glacial lake outburst flood process chain: the case of Lake Palcacocha and Huaraz, Peru. *Hydrol. Earth Syst. Sci.* **20**, 2519–2543 (2016).
13. Rivas, D. S., Somos-Valenzuela, M. A., Hodges, B. R. & McKinney, D. C. Predicting outflow induced by moraine failure in glacial lakes: the Lake Palcacocha case from an uncertainty perspective. *Nat. Hazards Earth Syst. Sci.* **15**, 1163–1179 (2015).
14. Lliboutry, L., Morales Arnao, B., Pautre, A. & Schneider, B. Glaciological problems set by the control of dangerous lakes in Cordillera Blanca, Peru. I. Historical failures of morainic dams, their causes and prevention. *J. Glaciol.* **18**, 239–254 (1977).

15. Emmer, A. Geomorphologically effective floods from moraine-dammed lakes in the Cordillera Blanca, Peru. *Quat. Sci. Rev.* **177**, 220–234 (2017).
16. Portocarrero Rodríguez, C. A. *The Glacial Lake Handbook: Reducing Risk from Dangerous Glacial Lakes in the Cordillera Blanca, Peru* (USAID, 2014); https://pdf.usaid.gov/pdf_docs/PBAAA087.pdf
17. Drenkhan, F., Huggel, C., Guardamino, L. & Haeberli, W. Managing risks and future options from new lakes in the deglaciating Andes of Peru: the example of the Vilcanota-Urubamba basin. *Sci. Total Environ.* **665**, 465–483 (2019).
18. Vilímek, V., Zapata, M. L., Klimeš, J., Patzelt, Z. & Santillán, N. Influence of glacial retreat on natural hazards of the Palcacocha Lake area, Peru. *Landslides* **2**, 107–115 (2005).
19. Frey, H. et al. Multi-source glacial lake outburst flood hazard assessment and mapping for Huaraz, Cordillera Blanca, Peru. *Front. Earth Sci.* **6**, 210 (2018).
20. Rabatel, A. et al. Current state of glaciers in the tropical Andes: a multi-century perspective on glacier evolution and climate change. *Cryosphere* **7**, 81–102 (2013).
21. Wegner, S. A. *Lo Que El Agua Se Llevó: Consecuencias y Lecciones del Aluvión de Huaraz de 1941* Tecnica 7 (Perú Ministerio del Ambiente, 2014).
22. Huggel, C. et al. Anthropogenic climate change and glacier lake outburst flood risk: local and global drivers and responsibilities for the case of lake Palcacocha, Peru. *Nat. Hazards Earth Syst. Sci.* **20**, 2175–2193 (2020).
23. Cochachin Rapre, A. & Salazar Checa, C. *Batimetría de la Laguna Palcacocha* (Ministerio de Agricultura y Riego, 2016); https://go.nature.com/3c4jpwC
24. Haustein, K. et al. A limited role for unforced internal variability in twentieth-century warming. *J. Clim.* **32**, 4893–4917 (2019).
25. Haustein, K. et al. A real-time Global Warming Index. *Sci. Rep.* **7**, 15417 (2017).
26. Allen, M. R. et al. in *Special Report on Global Warming of 1.5 °C* (eds Masson-Delmotte, V. et al.) 47–92 (WMO, 2018).
27. Morice, C. P., Kennedy, J. J., Rayner, N. A. & Jones, P. D. Quantifying uncertainties in global and regional temperature change using an ensemble of observational estimates: the HadCRUT4 data set. *J. Geophys. Res. Atmos.* **117**, D08101 (2012).
28. Cowtan, K. & Way, R. G. Coverage bias in the HadCRUT4 temperature series and its impact on recent temperature trends. *Q. J. R. Meteorol. Soc.* **140**, 1935–1944 (2014).
29. Gurgiser, W., Marzeion, B., Nicholson, L., Ortner, M. & Kaser, G. Modeling energy and mass balance of Shallap Glacier, Peru. *Cryosphere* **7**, 1787–1802 (2013).
30. Meier, M. F. & Tangborn, W. V. Net budget and flow of South Cascade Glacier, Washington. *J. Glaciol.* **5**, 547–566 (1965).
31. Kaser, G., Fountain, A. & Jansson, P. *A Manual for Monitoring the Mass Balance of Mountain Glaciers with Particular Attention to Low Latitude Characteristics* (UNESCO, 2003).
32. Sagredo, E. A., Rupper, S. & Lowell, T. V. Sensitivities of the equilibrium line altitude to temperature and precipitation changes along the Andes. *Quat. Res.* **81**, 355–366 (2014).
33. Malone, A. G. O., Doughty, A. M. & Macayeal, D. R. Interannual climate variability helps define the mean state of glaciers. *J. Glaciol.* **65**, 508–517 (2019).
34. Vuille, M. et al. Climate change and tropical Andean glaciers: past, present and future. *Earth Sci. Rev.* **89**, 79–96 (2008).
35. Kaser, G. Glacier–climate interaction at low latitudes. *J. Glaciol.* **47**, 195–204 (2001).
36. Stuart-Smith, R. F. *Melt Rate of Palcaraju Glacier, Cordillera Blanca, Peru: Attribution of Anthropogenic Influence and Proposed Methodology for Calculating Adaptation Cost.* FHS dissertation (Univ. Oxford, 2019).
37. Rohde, R. et al. A new estimate of the average earth surface land temperature spanning 1753 to 2011. *Geoinfor. Geostat.* **1**, https://doi.org/10.4172/2327-4581.1000101 (2013).
38. Poli, P. et al. ERA-20C: an atmospheric reanalysis of the twentieth century. *J. Clim.* **29**, 4083–4097 (2016).
39. Oerlemans, J. *Glaciology and Quaternary Geology* Vol. 6, 353–371 (Springer, 1989).
40. Medwedeff, W. G. & Roe, G. H. Trends and variability in the global dataset of glacier mass balance. *Clim. Dyn.* **48**, 3085–3097 (2017).
41. Hannart, A., Pearl, J., Otto, F. E. L., Naveau, P. & Ghil, M. Causal counterfactual theory for the attribution of weather and climate-related events. *Bull. Am. Meteorol. Soc.* **97**, 99–110 (2016).
42. Jomelli, V. et al. Fluctuations of glaciers in the tropical Andes over the last millennium and palaeoclimatic implications: a review. *Palaeogeogr. Palaeoclimatol. Palaeoecol.* **281**, 269–282 (2009).
43. Georges, C. 20th-century glacier fluctuations in the tropical Cordillera Blanca, Peru. *Arct. Antarct. Alp. Res.* **36**, 100–107 (2004).
44. Kaser, G. & Georges, C. Changes of the equilibrium-line altitude in the tropical Cordillera Blanca, Peru, 1930–50, and their spatial variations. *Ann. Glaciol.* **24**, 344–349 (1997).
45. Raetzo, H., Lateltin, O., Bollinger, D. & Tripet, J. P. Hazard assessment in Switzerland—Codes of Practice for mass movements. *Bull. Eng. Geol. Environ.* **61**, 263–268 (2002).
46. Wang, W., Yao, T., Gao, Y., Yang, X. & Kattel, D. B. A first-order method to identify potentially dangerous glacial lakes in a region of the southeastern Tibetan Plateau. *Mt. Res. Dev.* **31**, 122 (2011).
47. Bolch, T. et al. Identification of potentially dangerous glacial lakes in the northern Tien Shan. *Nat. Hazards* **59**, 1691–1714 (2011).
48. Haeberli, W. Mountain permafrost—research frontiers and a special long-term challenge. *Cold Reg. Sci. Technol.* **96**, 71–76 (2013).
49. Kinzl, H. & Schneider, E. *Cordillera Blanca (Perú)* (Univ. Wagner, 1950).

Methods

Temperature data and lack of precipitation trend. Given the minimal seasonal temperature variations and consequent year-round ablation from tropical glaciers[29,35], we modelled the evolution of Palcaraju glacier in response to annual mean temperatures. We primarily used the UK MetOffice HadCRUT4-Cowtan/Way (HadCRUT4-CW) dataset[27,28] as it provides continuous observations since 1850 and therefore a better pre-industrial baseline temperature for Peru than those of other observational datasets. Of the datasets considered, it also has an interannual temperature variability closest to the observed one. The standard deviation of annual mean temperature at the closest high-altitude meteorological station with an adequate record (the Mayor General FAP Armando Revoredo Iglesias Airport, 2,700 m) is 0.62 K compared with 0.64 K for HadCRUT4-CW over the same period (1963–2018).

The baseline temperature was taken as the mean of 1850–1880. The observed warming between the baseline and most recent 10 yr period (2009–2018) in HadCRUT4-CW is 1.01 K. Station observations in the Tropical Andes give temperature trends of +0.31 K per decade for 1969–1998 and +0.13 K per decade for 1983–2012[50]. Given these observed trends and the amplification of warming at higher altitudes[51] (the mean elevation of the HadCRUT4-CW grid cell is 1,333 m), it is likely that our estimate of regional warming in the HadCRUT4-CW dataset is conservative. These factors do not affect the proportion of the trend attributable to anthropogenic influence. Further, surface-temperature simulations from the Hadley Centre regional climate model version 3P (HadRM3P) coupled to the global atmosphere model HadAM3P from the weather@home distributed climate modelling system[52] give a temperature difference of around 1.5 K between the present and counterfactual (excluding human influence) climate (results not shown here).

A reduction in the HadCRUT4-CW variability is evident prior to 1940 (Fig. 2a) and probably reflects a greater reliance on interpolation over this period. The number of observations in the grid cell increases considerably from 1940, so this is the period regressed against the GWI. Regional anthropogenically forced warming above the 1850–1880 baseline was calculated for 1989–2018 as equalling 95% (85–105%, 5–95% range) of the observed temperature change. This value displays a slight sensitivity to the choice of the present-day period. If a period of ten years is used, following Allen et al.[26], regional anthropogenically forced warming equals 120% (105–135%, 5–95% range) of the observed value. The regression onto a global index assumes that the proportional contributions of anthropogenic and natural forcing to temperature change are the same at regional and global scales, justified by the absence of independent local factors that could create century-scale local climate trends. Such factors might include volcanic activity with effects localized to the Peruvian climate or substantial local changes in albedo due to land-cover alterations over the past 150 years. No such factors are known in this region[53].

We generated uncertainty estimates for the anthropogenic contribution to the temperature trends by regressing control simulations of 41 CMIP5 models (with no trends) against the GWI to calculate region-specific scaling factors for GWI. The product of GWI and these scaling factors creates a PDF of the degree that natural variability can project onto the observed temperature trend. The 5–95% range of this PDF is the uncertainty in our estimate of the anthropogenic influence. We note that temperature variability may be higher at the local scale than that simulated in CMIP5. However, in the Cordillera Blanca, the magnitude of interannual variability at grid scale and station data has been found to be similar over a 30 yr period[54]. Further, even given an extreme assumption that local interannual temperature variability is double that of the CMIP5 grid cell, the 5–95% confidence range in the attribution statement broadens only slightly, from 85–105% to 70–120%.

We took annual precipitation values as the accumulation zone mass balance (for 2006–2008) from the nearby Shallap glacier[29]. Previous studies found that most individual meteorological stations do not show significant trends in precipitation over the twentieth century[34], although some have found an increasing trend in Cordillera Blanca precipitation in recent decades[50]. This glacier is also comparatively insensitive to variations in precipitation (discussed further below) and we did not apply a precipitation trend here.

Interannual variability in temperature and precipitation, and persistence. The HadCRUT4-CW temperature dataset gives a standard deviation of 0.55 K in annual mean temperature for between 1880 and 2018, and the Legates and Wilmot precipitation dataset[55] gives a standard deviation of 0.2 m yr^{-1} in annual mean precipitation (1900–2010, with no significant trend)[55]. We tested for interannual persistence in the climate data using autoregression modelling[56]. The precipitation data are consistent with no persistence (that is, white noise) but, for the HadCRUT4-CW temperature data, the best-fit autoregressive process is a first-order (that is, AR(1)) process with a lag-1 correlation coefficient of 0.32, which indicates a decorrelation time of around a year. This persistence is probably associated with the influence of El Niño. Our synthetic time series of stochastic climate variability includes this persistence, which enhances the magnitude of natural glacier variability[2]. We also applied the autoregression model to an ensemble of 41 models of CMIP5 control runs and found lesser levels of persistence than observed in almost all models. As interannual persistence

enhances the natural variability against which we compare the retreat of Palcaraju glacier, the modelled persistence in CMIP5 suggests our incorporation of interannual persistence is a conservative assumption.

Vertical profile of mass balance. The influence of precipitation on the vertical mass-balance profile is incorporated in our modelling by using the observed mass-balance profile from Shallap glacier (with a similar aspect to that of Palcaraju). Gurgiser et al.[29] reported a vertical mass-balance gradient below the ELA (b_z^l) of approximately 3 m of water equivalent per 100 m. The vertical mass-balance gradient above the ELA (b_z^u) is approximately zero and the mass balance tapers smoothly to a constant of approximately 1.25 m of water equivalent per year. We join these two domains smoothly with a tanh function of altitude, z:

$$\frac{db}{dz} = b_z^l + \frac{(b_z^u - b_z^l)}{2}\left[1 + \tanh\left(\frac{z - z_{ELA}}{\delta z}\right)\right] \tag{1}$$

where z_{ELA} is the ELA and δz is the width of the transition zone (set as 200 m). $b(z)$ is then obtained by integrating equation (1) downwards from the top of the domain. Gurgiser et al.[29] report an ELA for Shallap of 4,985 m for 2006–2007 and 4,953 m for 2007–2008, in close agreement with the modern ELA we used for Palcaraju (Fig. 2a,b).

Tropical glaciers typically experience precipitation during the ablation season, and frequent changes in snow cover drive strong vertical gradients in albedo, and therefore mass balance[57]. The long ablation season of tropical glaciers also contributes to the strong vertical mass-balance gradient[35,57], which is nearly constant from year to year. Over two years of observations from the nearby Shallap glacier, Gurgiser et al.[29] reported only a 3% difference in the vertical gradient of the mass balance of the ablation zone, despite a 35% variation in accumulation. Consistent gradients can also be seen, for example, over 10 yr at Uruashraju in Peru[35], with similar results found for Zongo glacier in Bolivia[58] and elsewhere in the tropics[59]. The near-constant year-on-year shape of the mass-balance profiles means that vertical and horizontal shifts of the mass-balance profile are a useful and efficient approximation to represent climate forcing[30,31,33].

Climate sensitivity of mass balance. Following refs. [33,35,60], the impact of temperature anomaly (T') is implemented by vertically shifting the mass balance by an amount $z' = T'/\Gamma$, where $\Gamma = 5.5 \times 10^{-3}$ K km^{-1} is the observed lapse rate[29,57]. We quantify the impact of a precipitation anomaly by adding a uniform anomaly to the mass-balance profile (a horizontal shift in Fig. 2b). The steep mass-balance gradient in the ablation zone means that mass-balance variability is almost entirely due to temperature fluctuations. The interannual standard deviation of the ELA is 102 m with precipitation and temperature variability included, and 100 m when precipitation variability is omitted. For the 1880 glacier profile (Fig. 3a) this translates to an interannual standard deviation in mass balance of 0.78 m yr^{-1} and 0.74 m yr^{-1}, respectively, when precipitation is, and is not, included.

Our calculations, provided in full in the Supplementary Information, show that the ELA rises by 180 m for a 1 K temperature rise, in line with Sagredo et al.[32] (180 m) and Kaser[35] (182 m). By contrast, a 10% increase in annual mean precipitation raises the mass balance by approximately 0.1 m yr^{-1}, equivalent to a 13 m decrease in ELA. Normalizing the results from other tropical glaciers in the published literature to this same mass-balance perturbation gave ELA decreases of 16 m (ref. [32]) or 8 m (ref. [35]). These ELA changes are much lower than those that result from a 1 K increase in temperature. Temperature trends are much more important than the conceivable precipitation trends for the ELA and mass balance of Palcaraju glacier.

We further note that the mass-balance sensitivity to precipitation is reduced by Palcaraju glacier's wet climate, which means that, unlike some tropical glaciers, sublimation contributes only a small portion of the mass budget. Drier glaciers with substantial sublimation tend to have a higher precipitation sensitivity[61,62]. Gurgiser et al.[29] reported that sublimation and evaporation accounts for about 10% of the ablation on Shallap glacier, consistent with the specific energy balance calculations of Rupper and Roe[62].

Catchment geometry. The geometry of the Palcaraju glacier catchment was obtained from Google Earth (Lake Palcacocha 9° 23′ 42″ S, 77° 22′ 42″ W, elevation 8.8 km). A central-catchment flowline was estimated to obtain a longitudinal profile of the topography. We replaced the lake surface in Google Earth with the observed lake bathymetry[13], and restored the topography of pre-1941 GLOF moraine at the end of the lake based on the reconstruction in Rivas et al.[13]. The resulting profile is shown in Fig. 3a. The profile does not remove the existing ice in the upper catchment, but as its thickness is only a few tens of metres[63], it has only a small effect on the profile. Ten approximately evenly spaced swaths along the profile were measured for the catchment width and symmetrized about the central flowline to produce the idealized planform catchment geometry, shown in the insets in Fig. 3a.

Numerical model. The numerical model is the same as that used in Roe and O'Neal[6], based on Oerlemans[64]. The numerical model calculates ice flow from the shallow-ice approximation and Glen's Flow Law, and can be expressed as a pair of equations that are a function of time, t, and distance along the flowline, x:

$$\frac{dh}{dt} = \frac{1}{w(x)}\frac{d}{dx}[w(x)F(x)] + b(x) \qquad (2)$$

$$F(x) = f_d\rho^3 g^3 h^5\left(\frac{dz_s}{dx}\right)^3 \qquad (3)$$

where h is ice thickness, w is flowline width, F is the downslope flux, b is the mass balance, f_d is the deformation constant, ρ is the ice density, g is gravity and dz_s/dx is the surface slope. Equations (2) and (3) constitute a non-linear diffusion equation, wherein the ice flux is a sensitive function of the glacier shape. This numerical model is a useful tool to evaluate the glacier profiles that are consistent with the landscape geometry and the rising ELA associated with the observed climate trend. It also provides a method to estimate the timescale of the glacier response. This response time controls both the magnitude of the natural glacier fluctuations and the glacier's response to a climate trend[5,65]. The flowline model does not incorporate the effect of debris cover, subglacial till or lake-terminus dynamics, which includes ice calving and thermal conduction. Glacier flow may also have altered the subglacial topography which, after the retreat, became the lake bathymetry. As such, the flowline model is not intended or expected to produce an exact simulation of the glacier's evolution.

To estimate the glacier-length response to natural climate variability, we generated 10 kyr of synthetic climate variability with the same statistical characteristics (variance and lag-1-year autocorrelation) as the observations. The resulting glacier-length fluctuations have a standard deviation of 235 m.

Location of the 1880 terminus. In the absence of direct observations, we estimated the late nineteenth century terminus position, L_0. For our model, L_0 is the also the terminus position in equilibrium with the long-term average pre-industrial climate. Centennial-scale fluctuations about this equilibrium position result from the glacier's response to interannual climate variability (Fig. 4a)[6,65,66]. Our estimate for the magnitude of natural fluctuations is $\sigma_L = 235$ m. L_0 was necessarily set back from the main terminal moraine as previous work has shown the moraine formed in the seventeenth century[15], and it has not since been overtopped by natural glacier length fluctuations. Reconstructions from elsewhere in the Peruvian Andes also indicate that glaciers had pulled back from their seventeenth century maxima by the late nineteenth century[42]. It is also unlikely that L_0 was adjacent to the 1940 position: this would require a larger natural variability for the glacier to have extended as far as the seventeenth century moraine, and these larger fluctuations would have taken the glacier further up the valley than the 1940 position, for which there is no evidence here or elsewhere in the region[15,42]. Glaciers with larger natural variability are also more sensitive to climate change[65], which implies an even more sensitive system than that modelled here. Finally, some glacial retreat in the Cordillera Blanca was observed as temperatures began to rise in the decades prior to 1940[14,42–44]. We therefore set $L_0 = 4{,}250$ m. This places Palcaraju glacier's nineteenth century terminus approximately $2\sigma_L$ from both the seventeenth century moraine and the 1940 position, which is consistent with the glacier fluctuating within this portion of the valley in the eighteenth and nineteenth centuries, but not outside of it (Figs. 3a and 4a). Placing L_0 halfway between the seventeenth century moraine and the 1940 moraine is conservative: it allows for the largest magnitude of natural variability and is consistent with the known bounds of the glacier and our direct modelling of σ_L. If the 1880 position of the terminus is placed substantially closer to the 1940 front (say, $L_0 < 4$ km), it also becomes difficult to reconcile that 1880 location with the approximately 40% increase in net ablation rates that accompanies the 0.25 K of anthropogenic contribution to the 1880 to 1940 warming, seen in the insets on Fig. 3.

Signal-to-noise ratio. A comprehensive uncertainty analysis of the change in glacier length that can occur from natural variability alone ($\Delta L|_{null}$) is possible. Roe et al.[2] used the property of the glaciers' amplification of the signal-to-noise ratio of climate change, and that the amplification is greatest at intermediate glacier response times, to show that:

$$\Delta L|_{null} = \sigma_L \times \gamma(t_0, \tau) \times s_b|_{null} \qquad (4)$$

where $\gamma(t_0,\tau)$ is an amplification factor that depends only on the duration of the change (t_0) and the glacier response time (τ), and $s_b|_{null}$ is the signal-to-noise ratio of the mass balance (b) due to the observed interannual variability (that is, $\Delta b/\sigma_b$). The glacier response time equals the characteristic ice thickness (H) in the ablation zone divided by the (negative) net mass balance at the terminus (b_t) and affects both the amplitude and rate of change of length possible over a given time period, t_0. For the glacier's 1880 geometry, we estimated the response time as $\tau = \frac{H}{-b_t} \approx 150\,\text{m}/3\,\text{m\,yr}^{-1} \approx 50\,\text{yr}$. We have model estimates of τ and σ_L, but they are uncertain. We represent uncertainty in τ with a gamma function with 95% confidence bounds of 25–75 yr (Fig. 4d). Similarly, for σ_L, we give 95% confidence bounds of 115–345 m (Supplementary Fig. 2c). $s_b|_{null}$ is taken from the observed interannual variability and follows the Student's t-distribution[2]. Through equation (4), these PDFs yield PDFs for trends of length 60 and 140 yr in the absence of a climate change (Fig. 4e,f).

Equation (4) is derived in Roe et al.[2] based on a three-stage model of glacier dynamics, whose parameters are governed by the glacier's geometry and climatic setting[65]. The model has been shown to accurately emulate glacier fluctuations in numerical models of ice-flow dynamics[65–67]. The three-stage model is linear, and

although we do not expect linearity to apply over the whole valley profile, our goal was to characterize the much smaller fluctuations due to natural variability. The synthetic mass balance time series we applied to the numerical model (Fig. 4a) is normally distributed, so the resulting glacier fluctuations are also approximately normally distributed, which supports the linearity approximation.

GLOF hazard assessment. We used two methods to identify dangerous glacial lakes. The method proposed by Wang et al.[46] was developed to assess settings in which the likely GLOF mechanism would be a moraine-overtopping wave induced by an ice avalanche, as is the case with Lake Palcacocha. The GLOF hazard is quantified using the glacier area, the distance between the lake and glacier terminus, the slope between the lake and glacier, the mean slope of the moraine dam and the glacier-snout steepness. As Lake Palcacocha is in direct contact with Palcaraju glacier, we followed Wang et al.[46] and used the gradient of the glacier snout, defined as the glacier area within a 500 m horizontal distance of the terminus, in place of the slope between the lake and glacier. The area of the glacier is taken from the Global Land Ice Measurements from Space database[68] (the value is for 2015). The mean slope of the moraine dam before and after the 1941 GLOF (for the pre-industrial and present-day calculations, respectively) was taken from Somos-Valenzuela et al.[12], and from the slope of the glacier snout from our model reconstructions of the 1880 and present-day glacier geometries. Our assessment gives the same numerical value for the present GLOF hazard as that of Emmer and Vilímek[11], using this methodology.

We supplemented these calculations with an independent assessment adapted from Bolch et al.[47]. This methodology uses 11 weighted stability parameters, which relate to characteristics of the lake, lake surroundings and adjacent glaciers, and the potential impact on downstream areas. The parameters were ranked according to their influence on GLOF occurrence. We excluded two parameters from our analysis (glacier terminus slope and glacier velocity) as our analysis concerns the present-day GLOF hazard and these factors are used to identify glacial lakes for which a future rapid expansion may occur, which increases the hazard. We recalculated the weight factors for the remaining nine parameters according to the method provided in Bolch et al.[47] (the values are provided in Supplementary Table 3), which also instructs that flash-flood risk is set to zero if a debris flow is expected. We estimated the nineteenth century lake area as approximately 150,000 m² based on our modelling estimates of glacial retreat prior to 1941 and the estimated area of 303,000 m² immediately prior to the 1941 GLOF[69]. The lake area was 518,000 m² in 2016[23]. This method assesses hazard as 'high' if the four most important factors apply or if a combination of factors that, combined, is equal to the sum of the weights of the four most important factors apply.

Data availability

All climate data (observations and reanalysis) that support the findings of this study are publicly available from the KNMI Climate Explorer (https://climexp.knmi.nl/), except the Mayor General FAP Armando Revoredo Iglesias Airport station data, which was downloaded from the Center for Climate and Resilience Research (University of Chile) Climate Explorer (http://explorador.cr2.cl/). All CMIP5 model data used in this study are available in public repositories, for example, https://esgf-node.llnl.gov/search/cmip5/. The model data used here are stored on the Natural Environment Research Council's (NERC) designated data centre for the atmospheric sciences, BADC (British Atmospheric Data Centre). The GWI data are available from https://www.globalwarmingindex.org/AWI/AWI_AR5_new_spreadsheet.xlsx.

Code availability

Code will be available upon request to the corresponding author.

References

50. Schauwecker, S. et al. Climate trends and glacier retreat in the Cordillera Blanca, Peru, revisited. *Glob. Planet. Change* **119**, 85–97 (2014).
51. Mackintosh, A. N., Anderson, B. M. & Pierrehumbert, R. T. Reconstructing climate from glaciers. *Annu. Rev. Earth Planet. Sci.* **45**, 649–680 (2017).
52. Guillod, B. P. et al. weather@home 2: validation of an improved land–regional climate modelling system. *Geosci. Model Dev.* **10**, 1849–1872 (2017).
53. Betts, R. Biogeophysical impacts of land use on present-day climate: near-surface temperature change and radiative forcing. *Atmos. Sci. Lett.* **2**, 39–51 (2001).
54. Hofer, M., Mölg, T., Marzeion, B. & Kaser, G. Empirical–statistical downscaling of reanalysis data to high-resolution air temperature and specific humidity above a glacier surface (Cordillera Blanca, Peru). *J. Geophys. Res.* **115**, D12120 (2010).
55. Legates, D. R. & Willmott, C. J. Mean seasonal and spatial variability in gauge-corrected, global precipitation. *Int. J. Climatol.* **10**, 111–127 (1990).
56. Box, G. E. P., Jenkins, G. M., Reinsel, G. C. & Ljung, G. M. *Time Series Analysis: Forecasting and Control* (Wiley, 2008).
57. Sicart, J.-E., Hock, R., Ribstein, P., Litt, M. & Ramirez, E. Analysis of seasonal variations in mass balance and meltwater discharge of the tropical Zongo Glacier by application of a distributed energy balance model. *J. Geophys. Res.* **116**, D13105 (2011).

58. Sicart, J. E., Ribstein, P., Francou, B., Pouyaud, B. & Condom, T. Glacier mass balance of tropical Zongo glacier, Bolivia, comparing hydrological and glaciological methods. *Glob. Planet. Change* **59**, 27–36 (2007).

59. Kaser, G. & Osmaston, H. A. *Tropical Glaciers* (Cambridge Univ. Press, 2002).

60. Kaser, G., Juen, I., Georges, C., Gómez, J. & Tamayo, W. The impact of glaciers on the runoff and the reconstruction of mass balance history from hydrological data in the tropical Cordillera Bianca, Perú. *J. Hydrol.* **282**, 130–144 (2003).

61. Mölg, T. & Hardy, D. R. Ablation and associated energy balance of a horizontal glacier surface on Kilimanjaro. *J. Geophys. Res. D* **109**, D16104 (2004).

62. Rupper, S. & Roe, G. H. Glacier changes and regional climate: a mass and energy balance approach. *J. Clim.* **21**, 5384–5401 (2008).

63. Farinotti, D. et al. A consensus estimate for the ice thickness distribution of all glaciers on Earth. *Nat. Geosci.* **12**, 168–173 (2019).

64. Oerlemans, J. An attempt to simulate historic front variations of Nigardsbreen, Norway. *Theor. Appl. Climatol.* **37**, 126–135 (1986).

65. Roe, G. H. & Baker, M. B. Glacier response to climate perturbations: an accurate linear geometric model. *J. Glaciol.* **60**, 670–684 (2014).

66. Roe, G. H. & Baker, M. B. The response of glaciers to climatic persistence. *J. Glaciol.* **62**, 440–450 (2016).

67. Christian, J. E., Koutnik, M. & Roe, G. H. Committed retreat: controls on glacier disequilibrium in a warming climate. *J. Glaciol.* **64**, 675–688 (2018).

68. Cogley, J. G., Kienholz, C., Miles, E. S., Sharp, M. J. & Wyatt, F. *GLIMS Glacier Database* (NSIDC, 2015); https://doi.org/10.7265/N5V98602

69. Mergili, M. et al. Reconstruction of the 1941 GLOF process chain at Lake Palcacocha (Cordillera Blanca, Peru). *Hydrol. Earth Syst. Sci.* **24**, 93–114 (2020).

Author contributions

All the authors planned the analyses, which R.F.S.-S. and G.H.R. performed. All the authors contributed to the interpretation of the results and to writing the manuscript.

Competing interests

The authors declare no competing interests.

Additional information

Supplementary information The online version contains supplementary material available at https://doi.org/10.1038/s41561-021-00686-4.

Correspondence and requests for materials should be addressed to R.F.S.-S.

Peer review information *Nature Geoscience* thanks the anonymous reviewers for their contribution to the peer review of this work. Primary Handling Editors: Stefan Lachowycz, Heike Langenberg, Tom Richardson.

Reprints and permissions information is available at www.nature.com/reprints.